Spatial and temporal evolution of stress and slip rate during the 2000 Tokai slow earthquake

Shin'ichi Miyazaki,[1,2] Paul Segall,[1] Jeffery J. McGuire,[3] Teruyuki Kato,[2] and Yuki Hatanaka[4]

Received 9 September 2004; revised 9 September 2005; accepted 9 December 2005; published 23 March 2006.

[1] We investigate an ongoing silent thrust event in the Tokai seismic gap along the Suruga-Nankai Trough, central Japan. Prior to the event, continuous GPS data from April 1996 to the end of 1999 show that this region displaced ~2 cm/yr to the northwest relative to the landward plate. The GPS time series show an abrupt change in rate in mid-June 2000 that continues as of mid-2005. We model this transient deformation, which we refer to as the Tokai slow thrust slip event, as caused by slip on the interface between the Philippine Sea and Amurian plates. The spatial and temporal distribution of slip rate is estimated with Kalman filter based inversion methods. Our inversions reveal two slow subevents. The first initiated in late June 2000 slightly before the Miyake-jima eruption. The locus of slip then propagated southeast in the second half of 2000, with maximum slip rates of about 15 cm/yr through 2001. A second locus of slip initiated to the northeast in early 2001. The depth of the slip zone is about 25 km, which may correspond to the transition zone from a seismogenic to a freely sliding zone. The cumulative moment magnitude of the slow slip event up to November 2002 is $M_w \sim 6.8$. We calculate shear stress changes on the plate interface from the slip histories. Stress change as a function of slip rate shows trajectories similar to that inferred for high-speed ruptures; however, the maximum velocity is 8 orders of magnitude less than in normal earthquakes.

Citation: Miyazaki, S., P. Segall, J. J. McGuire, T. Kato, and Y. Hatanaka (2006), Spatial and temporal evolution of stress and slip rate during the 2000 Tokai slow earthquake, *J. Geophys. Res.*, *111*, B03409, doi:10.1029/2004JB003426.

1. Introduction

[2] The Nankai Trough, where the Philippine Sea Plate is subducting beneath southwest Japan at an annual rate of about 65 mm/yr [*Heki et al.*, 1999], has been the site of M ~8 class earthquakes every 100–200 years over the last 1000 years [e.g., *Ando*, 1975; *Sangawa*, 1993; *Kumagai*, 1996]. The 1944 Tonankai and the 1946 Nankaido earthquakes are the most recent such events. However, no major earthquake has occurred east of the 1944 Tonankai earthquake since 1854 when the entire Suruga-Nankai Tough is believed to have ruptured [e.g., *Ando*, 1975]. Hence this area is often referred as the Tokai seismic gap [e.g., *Ishibashi*, 1981]. Many studies have investigated whether the next large event is more likely to be a single event that occurs independently of the next Tokankai-Nakaido earthquakes or would occur within a few years of them.

[3] The Tokai district is located near a triple junction between the Amurian (southwest Japan), the North American (northeast Japan), and the Philippine Sea Plate (Figure 1). The development of a dense array of Global Positioning System (GPS) receivers has helped to determine the deformation pattern in this area. *Sagiya* [1999] used velocities of GPS stations between January 1997 and March 1999 to infer the state of plate locking at the Suruga-Nankai Trough in terms of slip deficit or "backslip," as introduced by *Savage* [1983]. *Sagiya* [1999] demonstrated that at depths of 10 ~ 20 km most of the fault had slip deficit rates as large as ~3–4 cm/yr, with a maximum slip deficit rate off Cape Omaezaki 138.36°E, 34.3°N, of ~4 cm/yr. He concluded, by comparing this to the rate of relative plate motion between the Eurasian and the Philippine Sea plates [*Seno et al.*, 1993], the plate interface must be fully locked at depths of 10 ~ 20 km.

[4] *Miyazaki and Heki* [2001] suggested that crustal deformation in the Tokai district can be separated into short-term elastic deformation caused by subduction of the oceanic plate and long-term deformation due to the interarc collision between southwest and northeast Japan. On the basis of their interpretation, *Heki and Miyazaki* [2001] decomposed the observed GPS velocity field between 1996 and 1999 into these two components and found that the long-term internal deformation of the landward plate, together with the westward rigid-block motion of a hypothesized Izu microplate, significantly influences the modeled slip rate on the Tokai segment of the Suruga-Nankai Trough. They estimated a slip deficit rate of ~2 cm/yr at the easternmost part of the trough at 138.5°E, 35.0°N, which is one third of that on the Nankai-Tonankai segments.

[1]Department of Geophysics, Stanford University, Stanford, California, USA.
[2]Earthquake Research Institute, University of Tokyo, Tokyo, Japan.
[3]Woods Hole Oceanographic Institution, Woods Hole, Massachusetts, USA.
[4]Geographical Survey Institute, Tsukuba, Japan.

Copyright 2006 by the American Geophysical Union.
0148-0227/06/2004JB003426$09.00

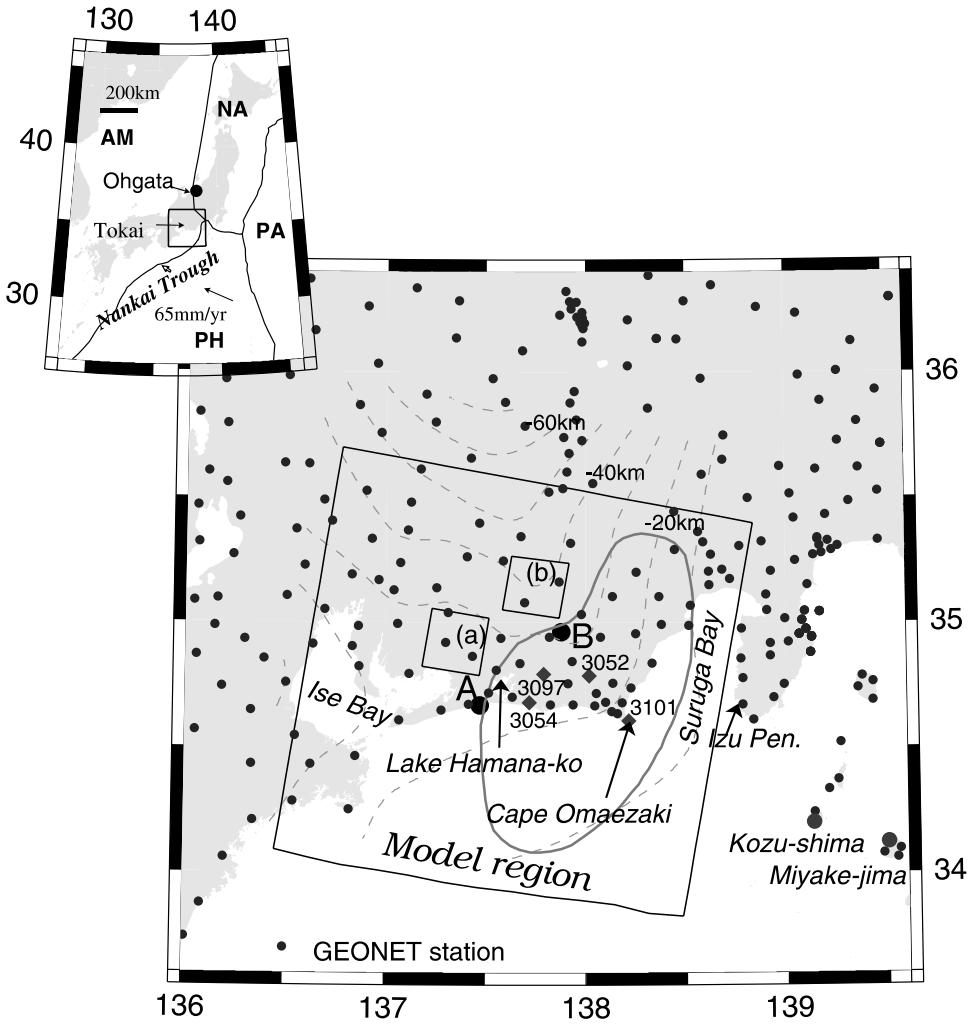

Figure 1. Tectonic settings of the Japanese islands. AM, PH, PA, and NA denote Amurian, Philippine Sea, Pacific and North American plates, respectively. Central Japan is overriding the Philippine Sea plate at the Suruga-Nankai Trough. The GEONET sites are marked with circles. The locations of specific GPS sites referred to in the text are noted. Model region is denoted with a rectangle; depth of the plate interface is contoured in kilometers. A and B are specific points referred to in the text. The a and b in parentheses indicate specific areas referred to in Figure 15. A ray closed line shows the anticipated source area of the next forthcoming Tokai earthquake proposed by *Central Disaster Management Council* [2001].

They concluded that this difference accounts for the longer recurrence intervals of interplate earthquakes in the Tokai seismic gap. Both *Sagiya* [1999] and *Heki and Miyazaki* [2001] found that the plate interface at the Suruga-Nankai Trough is strongly coupled and may cause a major event.

[5] *Ozawa et al.* [2002] reported an abrupt change in the rate of crustal deformation in the western Tokai area, from late 2000 or early 2001, about 3–6 months after the onset of volcanic activity on Miyake-jima island in early June 2000 [e.g., *Nishimura et al.*, 2001; *Toda et al.*, 2002]. *Kimata and Yamauchi* [1998] suggested that baseline shortening rates in the Tokai area may have decayed between 1987 and 1992. This possibly episodic event, which we refer to as the Tokai slow thrust slip event or Tokai slow slip for short, is currently ongoing [*Geographical Survey Institute*, 2004]. According to numerical simulations of earthquake cycles in the Tokai area, based on a rate- and state-dependent friction law [e.g., *Kato and Hirasawa*, 1999; *Kuroki et al.*, 2002], precursory slip should accelerate in the deepest portion of seismogenic zone. Hence it is important to infer the evolution of the slip distribution, not only for a better understanding of the earthquake generation process, but also to aid seismic hazard estimation in the Tokai seismic gap.

[6] *Ozawa et al.* [2002] modeled the deformation as resulting from departures in the amount of plate coupling at the Suruga Trough by employing Kalman filter methods based on the approach of *Segall and Matthews* [1997] for the period from September 2000 to June 2002. Further analysis of these data is warranted for several reasons. First, we wish to resolve whether or not there is a temporal correlation between the onset of the slow slip event and the Miyake-jima eruption, thus indicating a possible trigger for the aseismic slip. An accurate determination of the timing of onset of the slow slip event is vital to our understanding of the initiation mechanism. To answer this question we must include data from early 2000, unlike

Ozawa et al. [2002], who analyzed data beginning three months after the onset of the eruption in September 2000. Further analysis of the data is also warranted because, while *Ozawa et al.* [2002] removed secular and seasonal terms from the GPS time series, it appears that their results still contain a yearly seasonal signal, although the observation period is too short to be conclusive. Finally, *Ozawa et al.* [2002] made some assumptions related to the GPS reference frame that require further investigation. They arbitrarily assumed that GPS station Ohgata 133.0°E, 33.0°N (see Figure 1) did not experience transient deformation and did not use the full variance-covariance matrix of the GPS solutions. It is well known that the solutions depend on the fiducial site if full covariance matrices are not used and geodetic monuments are known to exhibit temporally correlated noise. For example, *Geographical Survey Institute* [2003] compared two solutions, one relative to Ogata, the second relative to Inagawa at 135.0°E, 35.0°N in southwest Japan, and found that they are significantly different.

[7] Slow slip events have now been observed worldwide, including the Bungo Channel, southwest Japan [*Hirose et al.*, 1999; *Ozawa et al.*, 2001; *Miyazaki et al.*, 2003; *Ozawa et al.*, 2004b], Cascadia, Pacific Northwest [*Dragert et al.*, 2001; *McGuire and Segall*, 2003; *Miller et al.*, 2002; *Rogers and Dragert*, 2003], San Juan Bautista, central California [*Linde et al.*, 1996], Parkfield, central California [*Murray and Segall*, 2005], Alaska [*Freymuller et al.*, 2002], Hawaii [*Cervelli et al.*, 2002] and Guerrero, southern Mexico [*Lowry et al.*, 2001; *Kostoglodov et al.*, 2003; *Larson et al.*, 2004; *Yoshioka et al.*, 2004].

[8] One notable feature of these first two examples is that the slow events occur repeatedly. Specifically, the Cascadia events occur at 14-month intervals [*Miller et al.*, 2002] with nonvolcanic tremor accompanying the slow slip events [*Rogers and Dragert*, 2003]. The Bungo Channel events have been observed in 1997 and 2003. *Obara et al.* [2004] and *Ozawa et al.* [2004b] found a clear correlation between these slow events and tremor activity. These phenomena may suggest that frictional properties are different in slow slip regions from those areas where high-speed rupture occurs. Several studies have attempted to estimate frictional properties for areas where high speed rupture occurred from seismic data [e.g., *Ide and Takeo*, 1997; *Guatteri et al.*, 2001; *Mikumo et al.*, 2003]. It is also important to estimate frictional properties for slow slip events to better understand what controls the speed of fault slip, which we try to address in this study.

[9] In the present study, we investigate the ongoing Tokai slow slip event to infer the history of slip from January 2000, well before the onset of a series of volcanic events on Miyake-jima and Kozu-shima islands, which is needed to resolve whether the slow event initiated before the eruption. We also extend the observation period up to November 2002, just before a systematic antenna/receiver replacement at the GPS stations. Our inversion method, an extended Network Inversion Filter, is based on an extended Kalman filter, which includes online estimation of temporal and spatial smoothing hyperparameters [*McGuire and Segall*, 2003]. We use loosely constrained GPS solutions with full covariance matrices [*Dong et al.*, 1998] to avoid any direct effect of the choice of fiducial site on the inversions. We also estimate slip and slip rate dependence of shear stress change to infer frictional properties on the fault surface.

2. Data and Preprocessing

2.1. Data

[10] We use continuous GPS data from the GPS Earth Observation Network (GEONET), operated by the Geographical Survey Institute (GSI), Japan [*Miyazaki et al.*, 1997; *Hatanaka et al.*, 2003]. As described in these studies, the number of stations is so large that it is not feasible to process all the data as one network. Hence the network is divided into subnetworks based on antenna and receiver types; each subnetwork is further divided into smaller regional subnetworks. The normal equations for the double-differenced GPS phase observables are then stacked for all regional clusters and constraints at the 0.1 mm level are imposed on the position of stations in Tsukuba to obtain the final solution. The combined solution with full covariance matrix is stored in the normal equation (NEQ) file format (Bernese specific binary format) at each combination step. Only the station positions, after fixing the Tsukuba stations, are distributed by GSI. The Tsukuba stations reveal unusual seasonal behavior due to groundwater level changes, as pointed out by *Munekane et al.* [2004], and these motions are propagated into the motions of all other stations. Previous studies such as the one by *Ozawa et al.* [2002] used this data set and are thus affected by these errors.

[11] It is preferable to use the full covariance matrix for the deformation analysis in order to take the correlation of measurements into account. We use NEQ files for the regional clusters before the final nationwide combination as the primary data set. Since the position of a selected station in each regional network is constrained at the 5 cm level, we first deconstrain the solutions and convert to quasi-observation (QOB) format, a software specific ascii format employed by the Quasi-Observation Calculation Analysis software (QOCA) [*Dong et al.*, 1998]. We then combine 14 days of QOB files using QOCA for each regional cluster. Finally we combine QOB files for all clusters and select 211 stations, mostly from around the Tokai area, with several remotely located stations to get a 14-day average data set (see Figure 2). We analyze a relatively large network since, as described later, we estimate network translation, rotation, and scale parameters together with fault slip to remove reference frame errors and remove rank deficiencies in the network. We use data between April 1996 and the end of 1999 to estimate the secular velocity and seasonal variations, and data between the beginning of 2000 and November 2002 for the Network Inversion Filter analysis of the Tokai slow slip event. We have not used data after December 2002 because GSI started to replace GPS antennae at that time, and to simultaneously change their analysis procedures.

2.2. Secular Velocities and Seasonal Variation

[12] We first estimate secular velocities and seasonal variations from GPS data between 1996 and 1999 and extrapolate these results to the data after January 2000 because the Tokai slow slip event and volcanism on Miyake-jima started in 2000. Because of the large number

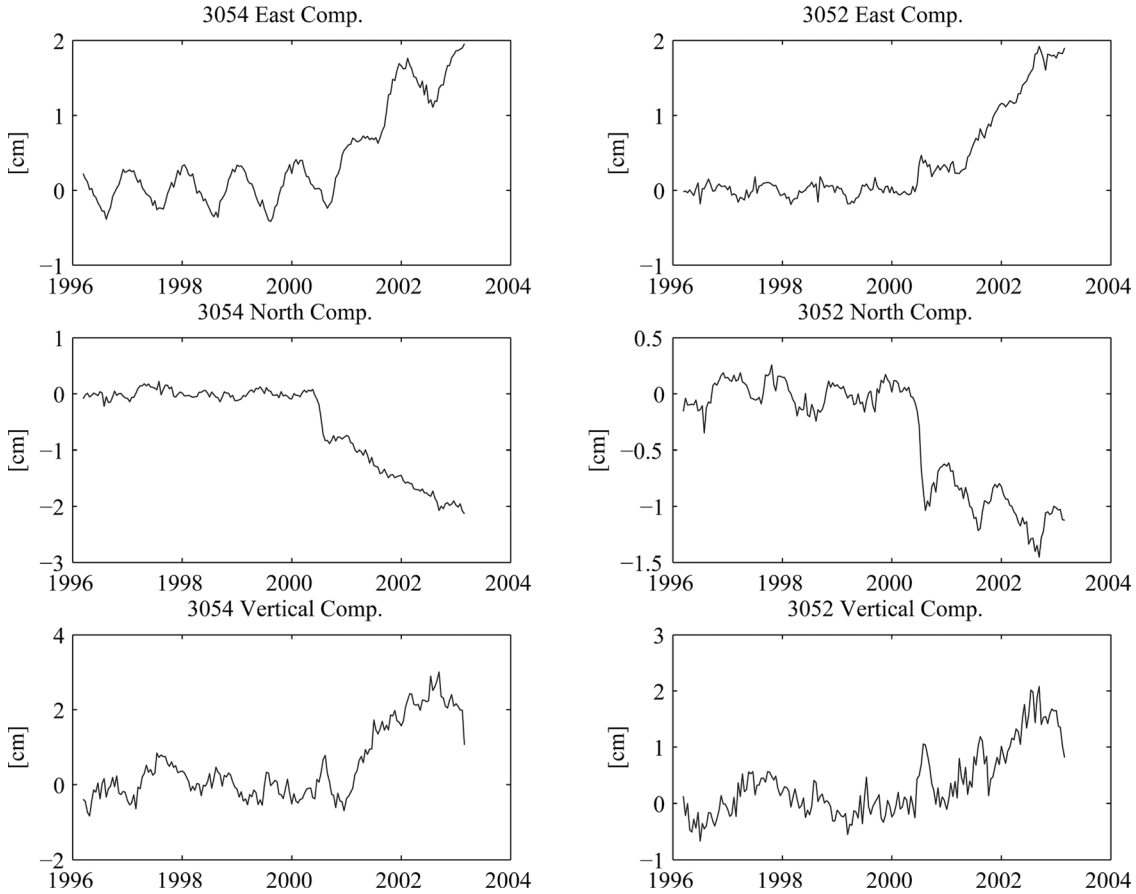

Figure 2. Raw GPS time series at selected stations, Hamamatsu (3054) and Kakegawa (3052). See Figure 1 for station locations.

of parameters, simultaneous estimation of the secular velocities and the transient motion was not computationally feasible.

[13] We employ the following observation model for the estimation of secular velocities and seasonal variation.

$$X(t) = X_0(t) + V(t - t_0) + Ff(t) + S_1 \sin(2\pi t) + C_1 \cos(2\pi t) + S_2 \sin(4\pi t) + C_2 \cos(4\pi t) + \epsilon(t) \quad (1)$$

where $X(t)$ is the position at observation epoch t, t_0 is the reference epoch, X_0 (t) is the position at the reference epoch t_0 and includes benchmark wobble at all other epochs t, V is the secular velocity, S_1, C_1, S_2, C_2 are the amplitudes of sinusoidal annual and semiannual variations, $f(t)$ is network translation, rotation, and scale, F is the Helmert matrix which relates $f(t)$ to the station positions, and $\epsilon(t)$ is measurement error. The measurement error is assumed to follow a normal distribution with mean zero and covariance $\sigma^2\Sigma(t)$. We estimate X_0 (t), V, $f(t)$, S_1, C_1, S_2, C_2 with a Kalman filter. The benchmark wobble is assumed to be random walk with a scale of 1 mm/$\sqrt{yr}$, and the reference frame parameter $f(t)$ is assumed to be white noise process with a large process noise (approximately meter level). All other parameters are assumed time invariant. The dimension of the state vector is 18 N_{sta} + 7 where N_{sta} is the number of GPS stations used in the filter (18 = 3 velocities, 3 benchmark terms, and 12 seasonal terms; 7 = 3 frame rotations, 3 translations, and network scale).

[14] If the secular deformation were steady and the seasonal variation purely periodic in time, the resultant data after the extrapolations would contain only nonsecular deformation. In fact the seasonal variation is not completely periodic, and reference frame corrections (Ff), and benchmark wobble (X_0 (t)) in our observation model in part account for departures from the idealized model. However, we cannot extrapolate the benchmark wobble or frame errors, only the secular and seasonal deformations. Thus the data we use in the subsequent Network Inversion Filter are

$$d(t) = X(t) - X_{ss}(t)$$
$$X_{ss}(t) = \hat{X}_0(t_0) + \hat{V}(t - t_0) + \hat{S}_1 \sin(2\pi t) + \hat{C}_1 \cos(2\pi t) + \hat{S}_2 \sin(\pi t) + \hat{C}_2 \cos(\pi t) \quad (2)$$

where $\hat{X}_0$, $\hat{V}$, $\hat{S}_1$, $\hat{C}_1$, $\hat{S}_2$, $\hat{C}_2$ represent the estimated values of initial positions, secular velocity and seasonal variations. We show examples of time series of $d(t)$ obtained by this procedure in Figure 3. *Murray and Segall* [2005] present a method for modeling quasiperiodic seasonal motions as annual sinusoids with slowly

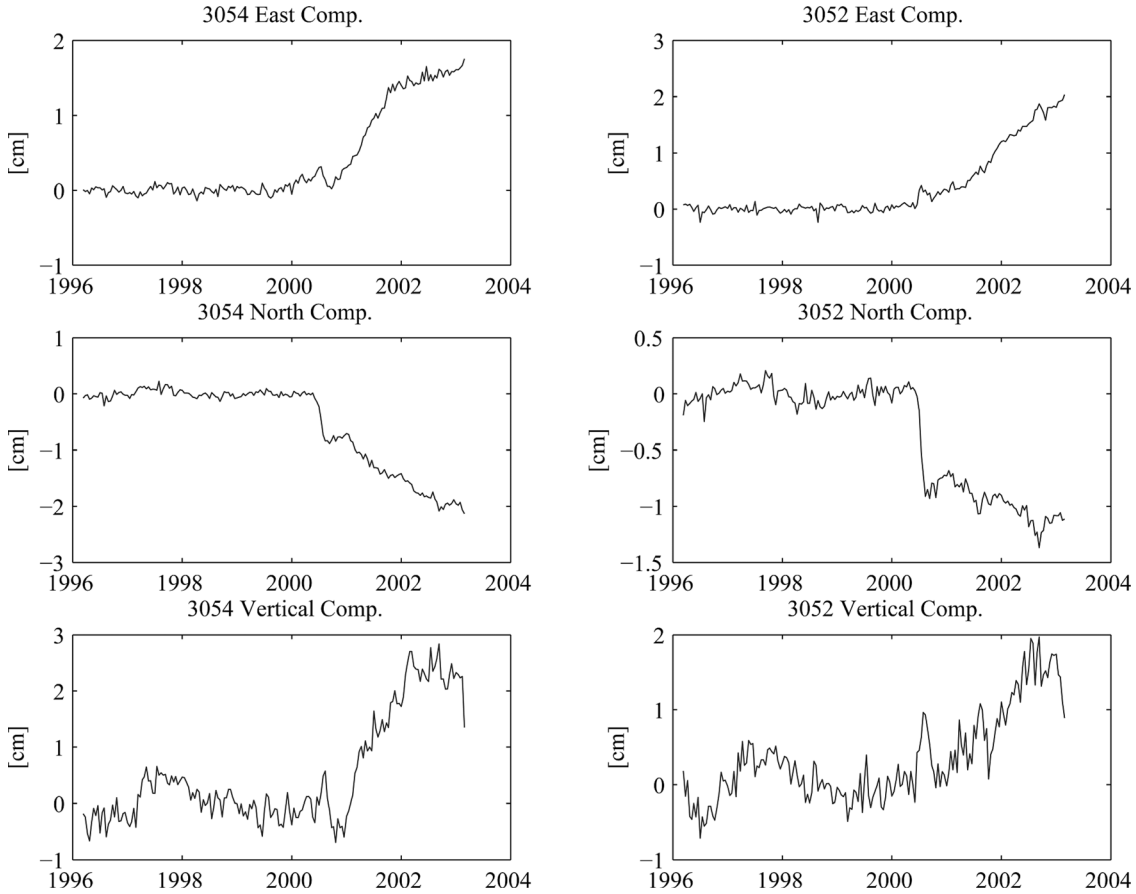

Figure 3. GPS time series for same sites as Figure 2, corrected for seasonal variations. Note that reference frame shifts are not removed from time series. See Figure 1 for station locations.

varying amplitude, however this approach is not well suite for the extrapolations here.

3. Plate Coupling Before the Tokai Slow Slip

[15] It is important to know whether slow events occur in strongly coupled regions of the fault and thus reduce the earthquake potential, or occur in weakly coupled regions, stressing the locked zones, and promoting the occurrence of future major events. This also relates to the distribution of frictional properties on the fault. If slow events never occur in strongly coupled regions, it would suggest that different frictional properties control the occurrence of slow and fast slip.

[16] The distribution of plate coupling along the Tokai segment of the Suruga-Nankai Trough inferred from inversion of GPS data [e.g., *Sagiya*, 1999] and clustering of seismicity [e.g., *Matsumura*, 1997] are significantly different. *Sagiya* [1999] inverted GPS velocities between 1996 and 1999 for the Suruga-Nankai Trough, and found that the highly coupled zone is located primarily offshore. On the other hand, *Matsumura* [1997] found a broad cluster of seismicity extending inland, west of Suruga Bay. On the assumption that those events occur inside the subducting oceanic crust and reflect the present stress state acting there, *Matsumura* [1997] hypothesized that they represent a stress concentration due to locking inland. The strongly coupled zone inferred by *Sagiya* [1999] is shallower than other parts of the Nankai Trough [e.g., *Ito and Hashimoto*, 2004]. To address this, and to have a consistent secular slip model to compare with the transient slip, we invert for the backslip distribution using the secular velocity determined from inversion of equation (1).

[17] *Sagiya* [1999] imposed smoothness constraints by minimizing the objective function $\Phi(s) = \|(d - Gs)\| + \gamma^2\|\nabla^2 s\|$ to stabilize his inversion, where d is data, s is slip, G is a matrix that contains the elastostatic Green's functions, ∇^2 is the Laplacian, and γ is the hyperparameter which represents the weight put on smoothing. The hyperparameter γ was optimized by minimizing Akaike's Bayesian Information Criterion (ABIC) [*Akaike*, 1980]. *Segall and Harris* [1987] point out, however, that minimum roughness norm solutions minimize the curvature in the slip, which could introduce slip offshore that is not required to fit the data while in minimum model norm inversions nearly all of the slip is found beneath the center of the geodetic network, and conclude it is better to compare both minimum model norm and roughness norms to determine what features are well resolved by the data. In the present study, we reexamine the slip deficit distribution using both minimum model norm and minimum roughness norms together in inversions of the GPS velocity field between 1996 and 1999. Instead of examining a range of solutions that vary the amount of smoothing, we optimized the solution by minimizing the ABIC.

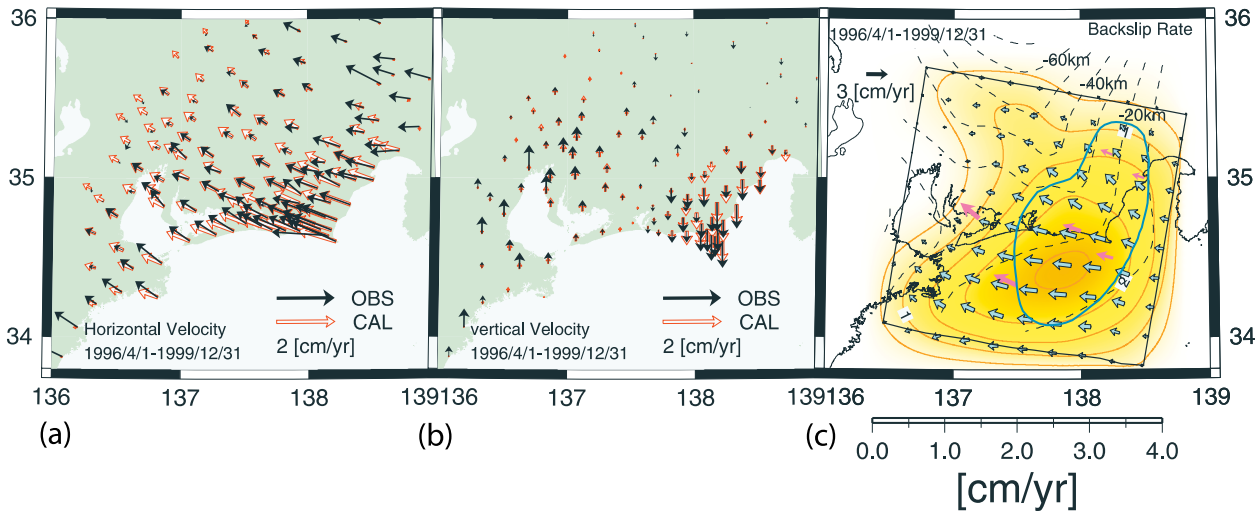

Figure 4. Steady deformation prior to the slow slip event inferred from GPS measurements made from 1996 to 1999. (a) Observed (black) and (b) predicted (red) velocities for horizontal and vertical motions. (c) Backslip distribution in the Tokai area. Blue arrows and contours show the backslip distribution, and red arrows are plate convergence rate from *Heki and Miyazaki* [2001]. Blue line shows the anticipated source area of the anticipated Tokai earthquake proposed by *Central Disaster Management Council* [2001].

[18] Following *Sagiya* [1999], we adopt the fault geometry of the Suruga-Nankai Trough estimated by *Yamazaki and Aoki* [1994] from the depth distribution of thrust earthquakes. *Sagiya* [1999] confirmed that there is no significant difference in using another fault configuration given by *Ishida* [1992]. We numerically integrate point source dislocations over subdivided fault patches, as has been done by *Yabuki and Matsu'ura* [1992] because of the complicated fault configuration. We take a 190 km × 190 km section of the fault as shown in Figure 1, subdivide it into 15 segments in both the strike and dip directions.

[19] Because the overriding plate is itself deforming [*Heki and Miyazaki*, 2001], we use GPS velocities in a relatively narrow area as shown in Figures 4a and 4b. We do not fix any stations, but rather estimate the relative velocity of the data frame (ITRF) and the reference frame defined by the dislocation model. The objective function to be minimized is $\Phi(s) = \|(d - Gs)\| + \gamma_1^2 \|\nabla^2 s\| + \gamma_2^2 \| s \|$, where d is data, s is slip, G is a matrix of elastostatic Green's functions, ∇^2 is the Laplacian, and γ_1 and γ_2 are hyperparameters which weight the smoothness and minimum norm constraints. Hyperparameters γ_1 and γ_2 are optimized by minimizing ABIC using a formulation given by *Fukahata et al.* [2004].

[20] The inferred distribution of slip rate deficit and the fit to the data are shown in Figure 4. We find that the maximum slip rate deficit is 2.5 ∼ 3.0 cm/yr, smaller than estimated by *Sagiya* [1999]. The uncertainty of the slip deficit is typically 3–4 mm/yr at depths greater than ∼20 km and 5–7 mm/yr at depths shallower than ∼20 km, reflecting the station distribution above the model region. We find the locus of slip deficit is deeper compared with the result of *Sagiya* [1999], but more consistent with the results of *El-Fiky and Kato* [2000] obtained from analysis of leveling data.

[21] Because of the complicated fault geometry and the model fault we have adopted, we do not account for shallow locking in the western part of the study area (136.5 ∼ 137.0°E). For this reason the predicted horizontal deformation is overestimated and uplift is underestimated in this region. Since we are interested in only the Tokai region, we accept the misfit in the west and adopt the backslip model for later discussion.

4. Method

4.1. Data and Inversion Method

[22] We use GPS data from the 360 stations shown in Figure 1. Prior to running the full Network Inversion Filter, we estimated the displacements due to the 2001 Hakone volcanic event using T. Nishimura's (personal communication, 2003) geometry and the 2002 Boso slow slip event using *Fukuda*'s [2003] geometry. Since those deformations are restricted to a small area and the durations are less than one month, we simply subtracted their contributions from the GPS data and did not estimate them in the following inversions. Also we subtracted coseismic displacements due to earthquakes in the Izu islands using *Nishimura et al.*'s [2001] dislocation model. Misfits which may appear from the use of those specific models would be accounted for by the benchmark wobble term.

[23] Deformation remaining in the GPS time series is associated with both the Tokai slow slip and the Miyake-Kozu volcanic events. Because the deformation is slow enough to assume quasi-static behavior, we use Volterra's equation. We use the same source geometry for the Tokai slow slip event as was used for the backslip inversion (see section 3), and fault geometries for the Miyake-Kozu volcanic events (Table 1) which follow *Nishimura et al.*

Table 1. Fault Parameters for the Miyake-jima Eruption[a]

	Latitude, deg	Longitude, deg	D, km	W, km	L, km	ϕ, deg	δ, deg	Type
1	34.137	139.373	0.5	10.0	12.7	125	90	T
2	34.225	139.254	6.3	6.7	14.5	128	90	T
3	34.214	139.191	1.3	14.0	5.4	96.3	89	S/D
4	34.146	139.371	7.5	1.4	7.8	182	91	S/D
5	34.067	139.521	4.2	-	-	-	-	M

[a]Latitude and longitude, position of the upper left edges of the fault planes; D, depth of the upper edge; W, width; L, length; ϕ, strike measured clockwise from the north; δ, dip angle; T, tensile; S, strike slip; D, dip slip; M, Mogi source.

[2001] and *Ozawa et al.* [2004a]. The observation model for the ith observation is

$$\begin{aligned} d_i(\mathbf{x},t) = & \int_{A^{(T)}} \mu\left[g^{(T)}{}_{ip,q}(\mathbf{x},\boldsymbol{\xi}) + g^{(T)}{}_{iq,p}(\mathbf{x},\boldsymbol{\xi})\right] s_p^{(T)}(\boldsymbol{\xi}, t-t_0) n_q^{(T)} \\ & \cdot(\boldsymbol{\xi}) dA^{(T)}(\boldsymbol{\xi}) + \int_{A^{(M)}} \left[\mu\{g^{(M)}{}_{ip,q}(\mathbf{x},\boldsymbol{\xi}) + g^{(M)}{}_{iq,p}(\mathbf{x},\boldsymbol{\xi})\}\right. \\ & \left. + \lambda\delta_{pq} g^{(M)}{}_{ir,r}(\mathbf{x},\boldsymbol{\xi})\right] s_p^{(M)}(\boldsymbol{\xi}, t-t_0) n_q^{(M)}(\boldsymbol{\xi}) dA^{(M)}(\boldsymbol{\xi}) \\ & + F_{ir}(\mathbf{x}) f_r(t) + B_i(\mathbf{x},t) + \epsilon_i(\mathbf{x},t) \\ \epsilon_i(\mathbf{x},t) \sim & N\left(0, \sigma^2 \Sigma_i(\mathbf{x},t)\right) \end{aligned} \tag{3}$$

where $\mathbf{d}(\mathbf{x}, t)$ is time series defined by (2), μ and λ are Lame constants, $g^{(T)}$ and $g^{(M)}$ are matrices of elastostatic Green's functions for Tokai slow slip ($^{(T)}$ = Tokai) and Miyake-Kozu events ($^{(M)}$ = Miyake-Kozu), where $g_{pq}(\mathbf{x}, \xi)$ is the displacement at $\mathbf{x}$ in the pth direction due to a force acting at ξ in the qth direction, $\mathbf{s}^{(T)}(\xi, t - t_0)$ and $\mathbf{s}^{(M)}(\xi, t - t_0)$ are slip on the Sagami-Nankai Trough and strength of the Miyake-Kozu sources, $\mathbf{n}^{(T)}(\xi)$ and $\mathbf{n}^{(M)}(\xi)$ are normal vectors to the area elements $A^{(T)}(\xi)$ and $A^{(M)}(\xi)$, respectively. A discrete approximation to the integrals in (3) is found by expanding the slip in two-dimensional B spline functions of order 3 following *Yabuki and Matsu'ura* [1992], so that the observation equation in the Kalman filter is cast solely in terms of matrix operations. As before, $F(\mathbf{x})\mathbf{f}(t)$ represents reference frame terms, $\mathbf{B}(\mathbf{x},t)$ is the Brownian benchmark motion, t_0 is the reference epoch, and $\epsilon(\mathbf{x},t)$ is unmodeled measurement error, assumed to be normally distributed.

[24] The fact that the Miyake-Kozu volcanic events occurred nearly simultaneously with the onset of the Tokai slow thrust slip present a serious challenge for the inversions, especially since both processes cause similar displacements along the coastal areas of the Tokai district. Displacement rates caused by the eruption were substantially higher than displacement rates associated with the slow slip event. Maximum opening rates associated with the volcanic deformation was ~100 m/yr, whereas the maximum slip rate for the slow slip event was ~0.14 m/yr. Because of the very different deformation rates the filter requires significantly less temporal smoothing for the volcanic processes than for the slow slip event. This of in itself would not be problematic, however an additional problem is that GPS data are not available for most stations on Miyake and Kozu islands from late August 2000 to late April 2001. When inverting for the Tokai slow slip and Miyake-Kozu volcanic processes simultaneously we find that the volcanic source parameters oscillate unrealistically during the period of missing observations. Because these deformations are so large they bias estimates of slip in the Tokai region.

[25] After considerable experimentation we have found that the most stable results are obtained by conducting the inversion in two steps. In the first step we model only the effects of Miyake-Kozu volcanic sources, $s_0^{(M)}$. Because we include stations on the Boso Penninsula northeast of the volcanic islands, that are not affected by the Tokai slow slip (see section 5), this step yields a reasonable first-order approximation to the volcanic deformation. In the second step we simultaneously invert for the Tokai slip $s^{(T)}$ as well as a correction to the Miyake-Kozu sources $s_1^{(M)}$. The final estimate of the Miyake-Kozu source parameters is $s^{(M)} = s_0^{(M)} + s_1^{(M)}$. The second inversion accounts for correlations between the volcanic and Tokai sources that would not be taken into consideration if we simply subtracted the predicted volcanic deformation from the data.

[26] More specifically, we first estimate only the Miyake-Kozu volcanic source parameters between June 2000 and June 2001 using an empirically determined temporal smoothing parameter

$$\alpha(t) = \alpha_0 \begin{cases} 0 & (t < t_0) \\ 1 & (t_0 \le t \le t_1) \\ 0.5 & (t = t_2) \\ 0.0005 & (t \ge t_3) \end{cases} \tag{4}$$

where t_0 = 2000/6/3 is one epoch before the onset of volcanic activity, t_1 = 2000/8/26 is the beginning of the missing observation period, t_2 = 2000/9/9 is the next epoch following t_1, and t_3 = 2000/9/23 is the epoch following of t_2. Note that the epoch interval is two weeks. A smaller smoothing parameter is used as the deformation gets smaller to prevent the solution from oscillating unphysically. The coefficient α_0 is optimized by maximum likelihood. We use the fault geometry shown in Table 1. Second, we estimate the Tokai slow slip event in addition to corrections to the Miyake-Kozu source parameters from the first step. Because the first-order effect of the eruption is accounted for in the first step, we can use a tighter temporal smoothing constraint in the second. This stabilizes the inversion and suppresses the bias of Tokai slow slip parameters caused by the mismodeling of the Miyake-Kozu parameters during the period of missing observations.

[27] We use an extended Kalman filter [*McGuire and Segall*, 2003], a modified version of the original Network Inversion Filter of *Segall and Matthews* [1997], which allows us to put temporal and spatial smoothing parameters (hyperparameters) into the state vector. The original extended filter implemented positivity constraints by introducing pseudo-observations and another hyperparameter, which increased the dimension of the state vector by the number of fault elements. In our case, this would have required an additional 451 parameters. To avoid such a large state vector, we use another implementation of positivity constraints proposed by *Simon and Simon* [2003] (also used by *Ozawa et al.* [2002]), which uses quadratic programming at each filter step, thus avoiding any extra parameters/hyperparameters.

4.2. Resolution of the Time-Dependent Inversion

[28] Fault slip inversions in offshore areas often suffer from poor spatial resolution. We examine the spatial resolution of

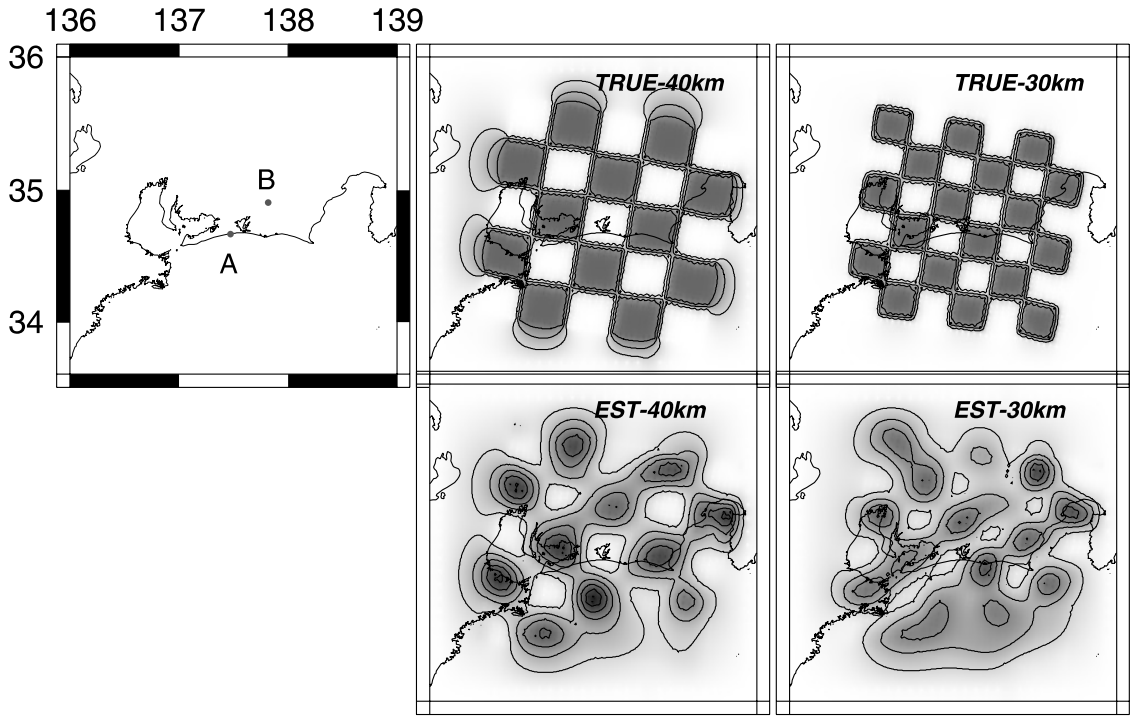

Figure 5. Spatial resolution of the time-dependent inversion. (middle and right) (top) "True" slip distributions and (bottom) inferred slip distributions from the inversion. Points A and B in Figure 5 (left) are referred to in Figure 6.

our inversions using synthetic slip distributions with the same fault geometry and station geometry as the actual data. The test distribution consists of a "checker board" pattern with square patches 30 km and 40 km on a side (Figure 5). The temporal evolution of slip rate in the N35°W direction is

$$\dot{s}(t) = \frac{1}{\sqrt{2\pi\sigma_0^2}} \exp\left[-\frac{1}{2\sigma_0^2}(t-t_0)^2\right] \tag{5}$$

where $\sigma_0 = 0.5$, $t_0 = 2001.5$. $s(t)$ is shown in Figure 6. To the calculated surface displacements we add Brownian benchmark wobble with $\tau = 1$ mm/$\sqrt{\text{yr}}$ and white noise of 2.5 mm in the horizontal and 10.0 mm in the vertical. Then we run the extended Network Inversion Filter to estimate the fault slip distribution and benchmark wobble.

[29] The estimated slip rate distribution at the final epoch is shown in Figure 5. (It is implied that the resolution changes very little from time step to time step because the network does not change.) As expected, the offshore area is poorly resolved. On the other hand, the inland area and coastal area up to ~30–40 km from the coast line are well resolved. Comparison of the cases with 30 and 40 km patches suggests that in the inland and coastal areas 40 km patches are well resolved and 30 km patches are also mostly resolved, while even 40 km patches are not resolved in the offshore areas. We compare the synthetic slip rate history with the estimated value at point A and B (see Figure 6) and find that the slip rate history is well resolved.

5. Results

[30] The Miyake-kozu events caused southeast directed displacements of up to several centimeters in the Tokai area, comparable to those due to the slow slip event, which may cause trade-offs between volcanic and tectonic sources of deformation. Hence we first show how effectively the inversion procedure is able to separate the two deformation sources.

[31] Figures 7a and 7b show the predicted displacements due to the Miyake-Kozu volcanic events and the Tokai slow slip event at the final epoch, respectively, together with observed displacements corrected for the Boso slow slip events, Hakone activity, coseismic steps, and reference frame shifts. Predicted displacements in the western Tokai area, Izu peninsula and Boso peninsula, and Izu islands are distinctly different for the volcanic and slow slip sources. These areas are key in distinguishing between the two different processes, despite the fact that both models predict southeastward displacements in the eastern Tokai region. Displacements on the Boso and Izu peninsulas are reproduced by the Miyake-kozu sources, while those in western Tokai are reproduced by the slow slip event. Finally, uplift of the Tokai area is not predicted by the Miyake-Kozu volcanic sources, but is well explained by the Tokai slow slip event. Thus we conclude that the data can distinguish between the various sources.

[32] Next we verified the consistency of our Miyake-Kozu source model with previously published results. Figures 8a and 8b illustrate the observed and predicted GPS displacements from our study (on 9 September 2000) and *Nishimura et al.* [2001], respectively. In spite of the difference in GPS station coverage, data period and inversion methods, the predictions of the two models are quite consistent. From these investigations, we conclude that the inversion can effectively distinguish between the magmatic process in the Miyake-Kozu area and the Tokai slow slip event.

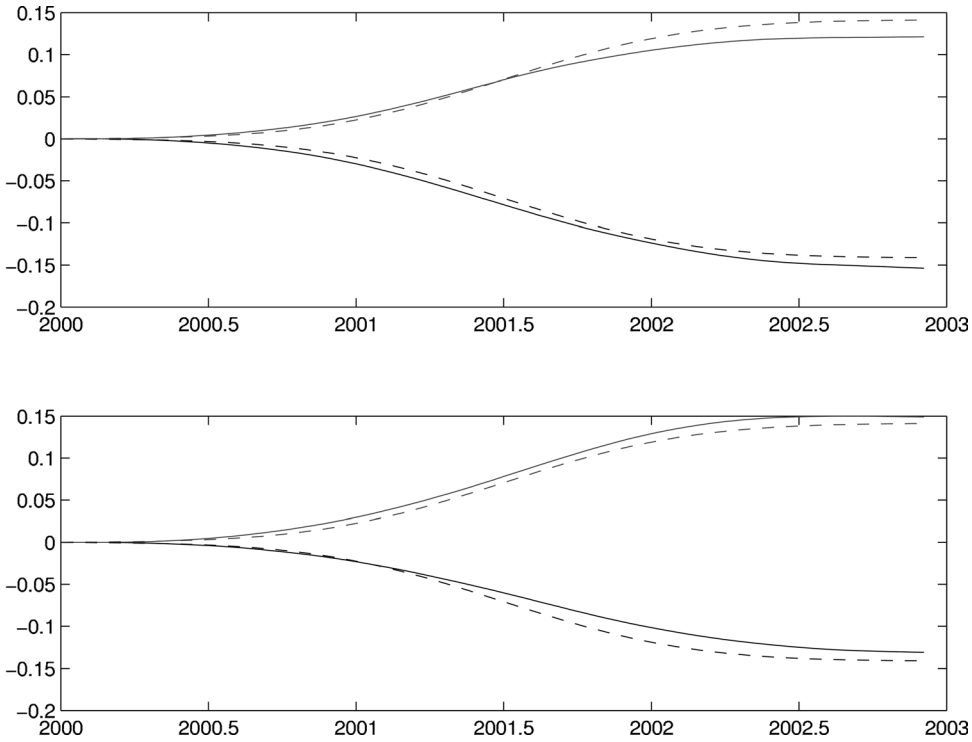

Figure 6. Temporal resolution of the time-dependent inversion. Cumulative slip history at (top) point A and (bottom) point B shown in Figure 5. Dashed lines are the "true" slip history, and solid lines are inferred from the inversion.

[33] Figure 9 shows observed and predicted displacement time series of selected GPS stations located in Figure 1. Contributions from the Miyake-Kozu events and reference frame shifts are subtracted from the observations, but the benchmark wobble term is left in. The predictions contain signals from the Tokai slow slip event only. The fit is reasonably good for stations in the Tokai area. Figures 10a and 10b show the observed and predicted displacement field for 1 January 2000 to 30 June 2001 and 1 July 2001 to 30 November 2002, respectively. Again, the observations are corrected for the volcanic deformation and reference frame shifts, and the predicted displacements include only the Tokai slow event. The fit to the observed velocity field is reasonably good, showing that estimated fault slip accounts for most of the non-secular deformation in the GPS time series.

[34] The estimated fault slip rate at the Suruga-Nankai Trough is shown in Figure 11 (an animated version is given in Animation S1 in the auxiliary material[1]). Each plot of Figure 11 represents a snapshot of slip rate at depth projected onto the Earth's surface. Uncertainties in the estimated slip rate are not shown for the sake of clarity but are typically ~3 cm/yr in segments deeper than 20 km and are nowhere greater than ~3.5 cm/yr.

[35] The slip rate is initially almost zero since we imposed a zero a priori transient slip rate. The estimated slip rate starts to exceed the uncertainty in mid-2000, slightly before the onset of the Miyake-Kozu volcanic events. The maximum slip rate is found around 137.3°E, 34.9°N at depths of between 25 and 30 km. The slip starts to migrate updip from August to October 2000 with the maximum slip rate moving to 137.5°E, 34.5°N. Slip then accelerates to ~14 cm/yr by April 2001. A second locus of slip initiates in January 2001, around 137.8°E, 35.3°N with slip rates of ~3 cm/yr. This locus also accelerates, and migrates updip to 137.8°E, 34.9°N from May to September 2001, while the first locus propagates slightly updip around 137.58°E, 34.6°N and starts to decelerate. The first locus decelerates further to ~3 cm/yr by the end of 2001. On the other hand, the second one continues to accelerate up to ~10 cm/yr by September 2002. Since then, this locus has decelerated, but continues to slide at ~10–15 cm/yr by the end of our study period. These results suggest that there are essentially two slip episodes, the first one possibly triggering the second. The cumulative nonsecular slip from 1 January 2000 to the end of November 2002 is displayed in Figure 12. The maximum value of slip reaches ~14 cm directed to the southeast, roughly opposite to the subduction of the Philippine Sea Plate. Typical uncertainties are ~7–10 mm at depths of $\geq$20 km and ~10–15 mm at depths $\leq$20 km. The zone of transient slip imaged offshore near 138.2°E, 34.0°N is almost certainly an artifact of the inversion since the spatial resolution in this area is poor (see Figure 5).

[36] Figure 13a shows the source time function at selected points (A and B shown in Figure 1). It may be observed from Figure 13 that the slip initiates earlier than mid-2000, then accelerates at A. The maximum slip rate at A is about 14 cm/yr, slip then decelerates by the end of 2001. Slip rate at B is not significant until early 2001, then keeps sliding at ~10 cm/yr in 2002. The cumulative moment for nonsecular slip at the final epoch,

[1] Auxiliary material is available at ftp://ftp.agu.org/apend/jb/2004jb003426.

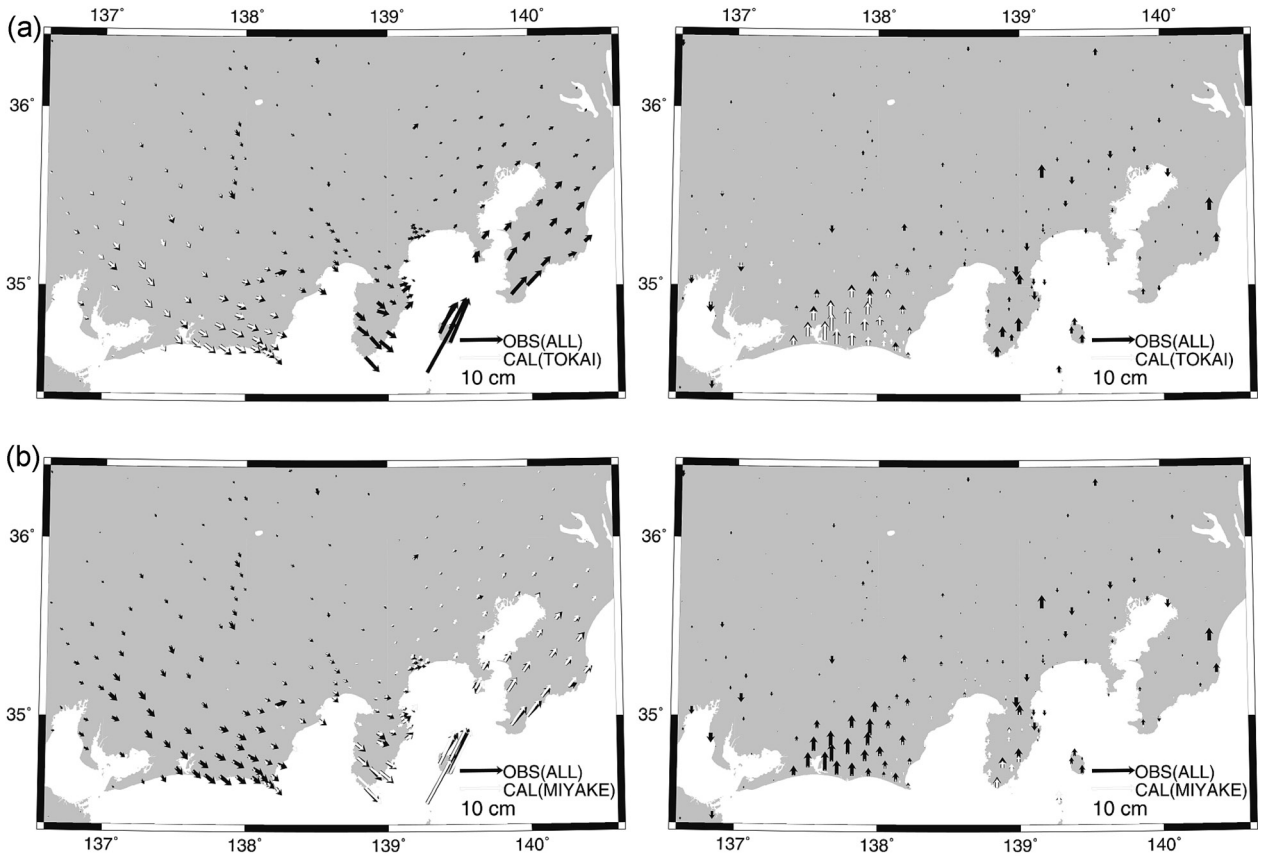

Figure 7. Predicted displacements for (a) the Tokai slow slip and (b) the Miyake-Kozu events for the entire analysis period (white arrows). Observed displacements for the same period (black arrows) contain signals from both the Tokai slow slip and Miyake-Kozu events. (left) Horizontal displacements and (right) vertical displacements.

30 November 2002, is $\sim 2.0 \times 10^{19}$ N m, which is equivalent to an earthquake of $M_w \sim 6.8$.

6. Implications for Fault Frictional Properties

6.1. Observational Constraints

[37] In order to better understand the physics of slow slip events, we investigate how the stress on the fault varies with slip and slip rate during the transient event. For this purpose, we compute the change in shear stress at the center of each patch on the plate interface during the slow slip event for our modeled slip, approximating the slip distribution with rectangular dislocations [*Okada*, 1992] whose patch size is $\sim$2.5 km, and assuming a rigidity of 30 GPa and Poisson's ratio of 0.25. Note that slip rate in Figure 13a is the departure from the secular velocities (the slip deficit is shown in Figure 4) while stress change as well as slip rate and cumulative slip in Figures 13b, 13c, and 13d includes the effect of both nonsecular and secular components. We find no significant difference from this result when we exclude the secular slip deficit in the stress calculations or when we adopt $\sim$5 km patches. Typical uncertainties are 3 $\sim$3.5 cm/yr for slip rate ($\sim$1.2 for log(slip rate) when slip rate is $\sim$5 cm/yr) and 0.7 $\sim$1.5 cm for slip ($4 \sim 10 \times 10^{-6}$ for the spatial derivatives of slip because the patch size used for stress calculation is $\sim$2.5 km). Hence the uncertainty in stress is of the order of $\sim$0.1 MPa to 0.2 MPa, assuming a shear modulus of 3×10^4 MPa.

[38] Shear stress change parallel to the direction of plate convergence is shown as a function of time in Figure 13b for two points (A and B) on the fault shown in Figure 1. Shear stress at A starts to decrease in the mid-2000, eventually dropping by 0.25 MPa in late 2001. Stress at B first increases due to slip around A, then starts to drop as slip increases in 2001.

[39] A stress-slip plot (Figure 13c) shows a linear decrease in stress with slip. This simply reflects the elastic unloading slope. Since the slip occurred quasi-statically the shear stress must always balance the frictional resistance. Ignoring plate motion the shear stress follows $\tau_0 - ku$, where k is an effective stiffness, so that the stress must decrease linearly with slip. There can be no critical slip beyond which strength is constant in this quasi-static system, for this would require the driving stress to drop below the strength.

[40] We also examine the dependence of shear stress on slip rate in Figure 13d. The slip rate at A initially increased at approximately constant shear stress. The shear stress then dropped at an approximately constant slip rate, and finally started to decelerate at nearly constant shear stress. At point B the shear stress initially increased due to loading from slip near point A. Following this, the two curves show similar

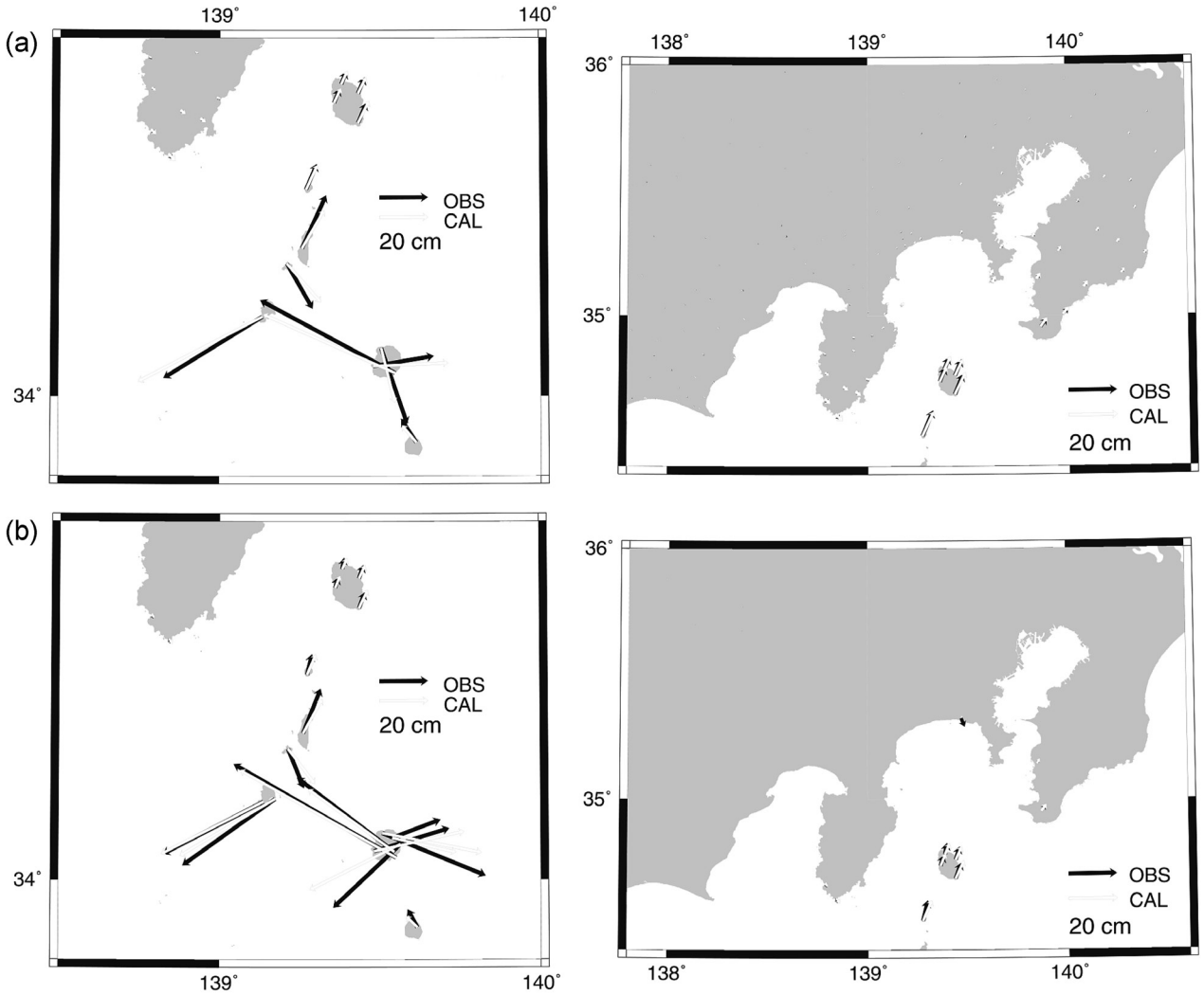

Figure 8. Predicted horizontal displacements for the Miyake-Kozu events (white arrows) obtained (a) in this study for the period 1 January 2000 to 9 September 2000 and (b) by *Nishimura et al.* [2001] as the differences between the average positions of 13–22 June 2000 to 27–31 August 2000. Observed displacements that were used for the version are shown by black arrows.

features. The stress-log(slip rate) paths are similar to that inferred for high speed ruptures except that the limiting velocity is not inertially controlled, and implies steady state velocity weakening friction including spontaneous slip nucleation and conditionally stable behavior [*Ruina*, 1983], as discussed later.

[41] It is interesting to compare this behavior with other transient events. Cascadia slow events, first found by *Dragert et al.* [2001], are different from the Tokai event in duration (3 months for Cascadia, more than 3 years for Tokai), cumulative slip amplitude (0.02 m for Cascadia, greater than 0.2 m for Tokai), maximum slip rate (1 m/yr for Cascadia, 0.13 m/yr for Tokai), moment magnitude ($M_w \sim$ 6.9 for Cascadia and greater than 6.8 for Tokai), and recurrence intervals (14 months for Cascadia [*Miller et al.*, 2002], 6–8 years for Tokai [*Kimata and Yamauchi*, 1998]). *McGuire and Segall* [2003] investigated the spatio-temporal variation in slip rate during the Cascadia slow slip event late 1999. We use their slip inversion to compute stress change for 2 points on the fault (Figure 14). The shear stress at A decreased by about 0.04 MPa between 1999.6 and 1999.7, was then reloaded by the slip around B. Stress at B started to drop at 1999.7 and decreased by ~0.06 MPa by the end of the analyzed period. Note that the general pattern of behavior is similar to the results for the Tokai events although the peak velocities are different, suggesting common frictional properties in those two slow slip areas.

6.2. Possible Mechanisms

[42] Hypotheses for the mechanics of slow earthquakes may be divided into two categories in terms of rate- and state-dependent friction [e.g., *Dietrich*, 1978; *Rice and Ruina*, 1983]. The first involves a change in the frictional behavior above a certain threshold slip velocity. The second involves spatial variation in the frictional properties. Specifically, in the first case the friction could be velocity weakening at low slip speeds but velocity strengthening at high speeds (due either to the intrinsic coefficient of friction or perhaps due to dilatancy). The second category involves spatial variations of constitutive parameters that cause

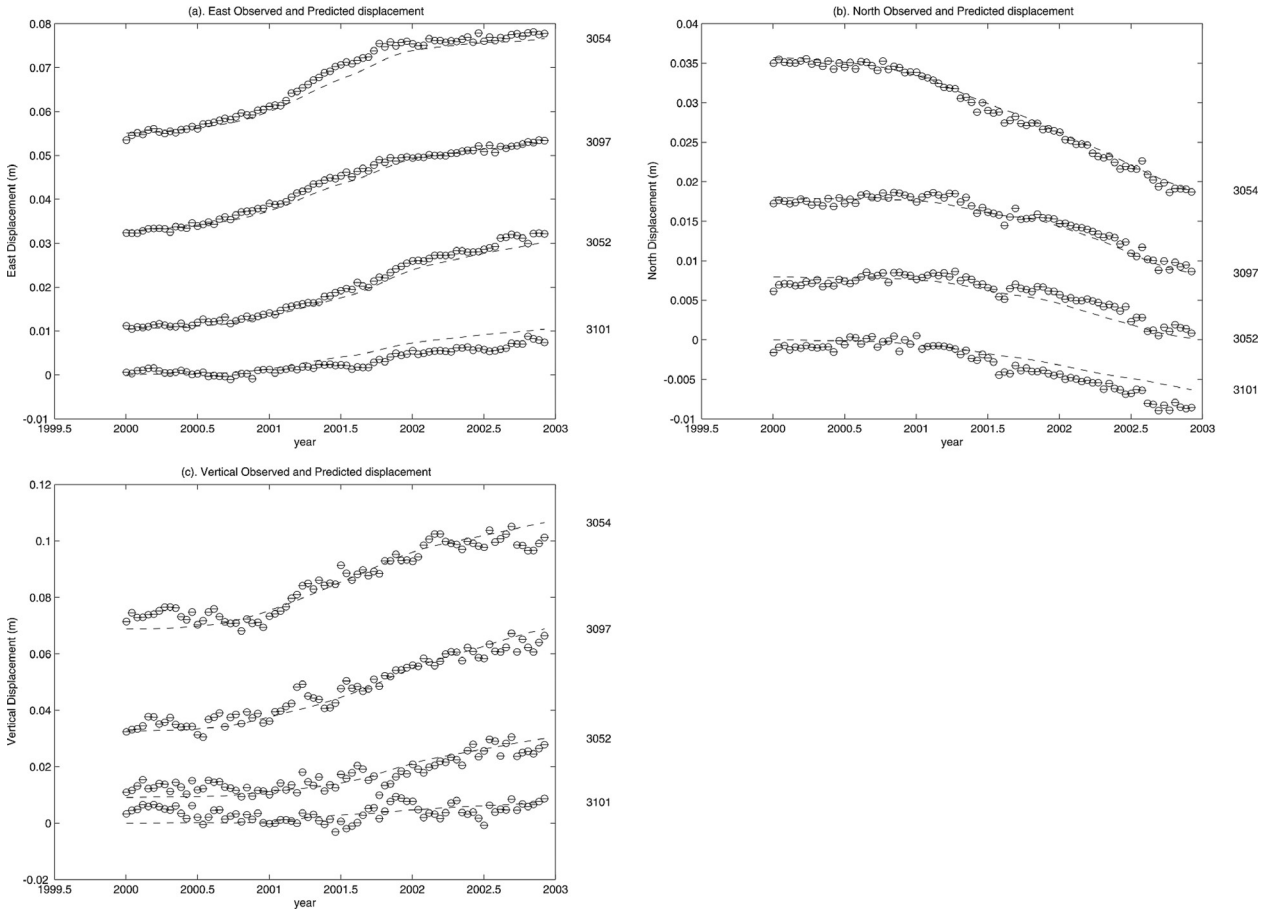

Figure 9. Fit to the data for selected stations. The data, shown as open circles, are corrected for Miyake-jima eruption and reference frame errors. The predicted signal components due to time-dependent fault slip are shown with a dashed line. Vertical axis is displacement, horizontal axis is time. (a) East components, (b) north components, and (c) vertical components. See Figure 1 for station locations.

hetelogeneous stress distribution and dynamic interactions that occur due to spatial variations in friction, which at any point is either weakening or strengthening. We might hope to be able to distinguish between these broad classes of mechanisms based on the resulting stress slip rate histories as in Figure 13d. We previously noted that the stress-log(slip rate) paths look similar to those for simple models of inertially driven slip instabilities [e.g., *Rice and Tse*, 1986].

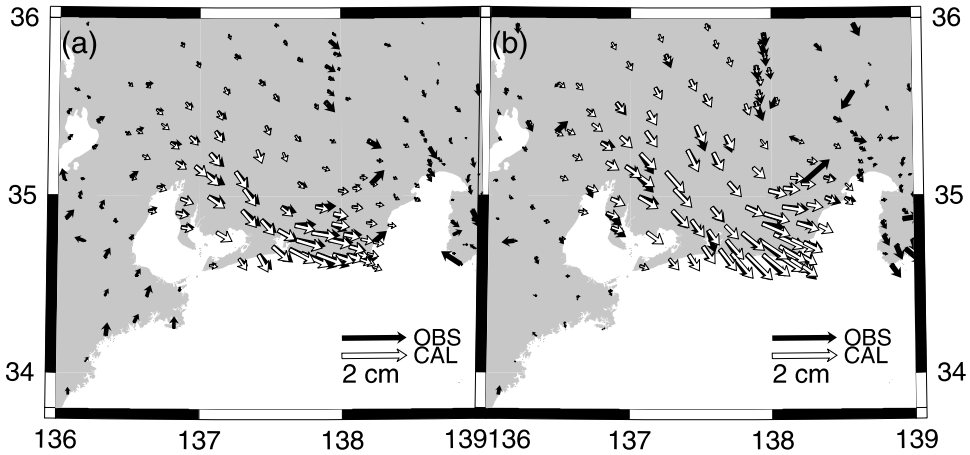

Figure 10. Time-dependent velocity field (shown as the departure from the secular velocity field.) Both observed (solid arrows) and predicted (open arrows) velocities are shown for the periods (a) 1 January 2000 to 30 June 2001 and (b) 1 July 2001 to 30 November 2002. Note that the random benchmark motion and reference frame errors are not included in the predicted velocity.

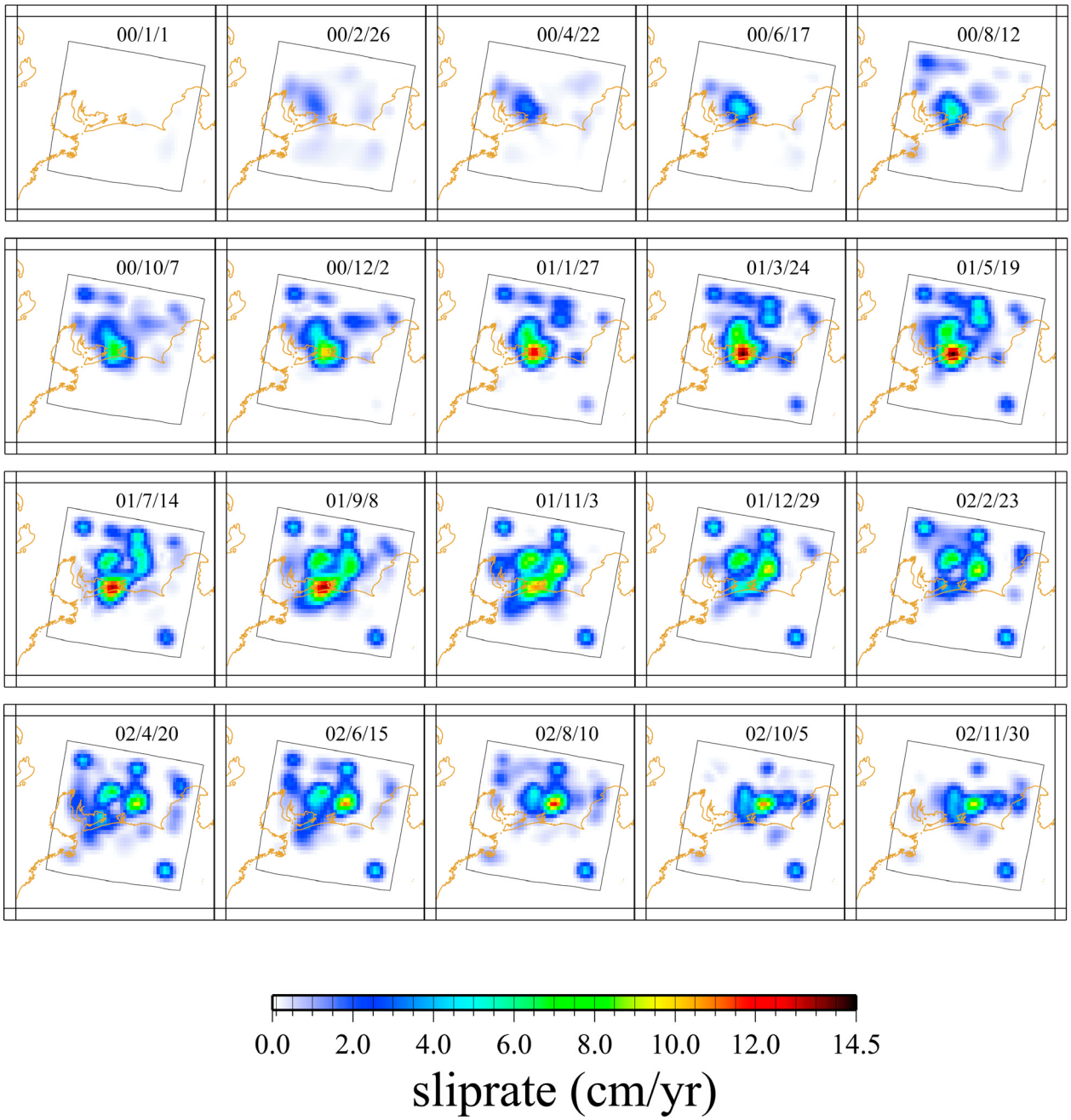

Figure 11. Space time evolution of slip rate on the plate interface at three-epoch intervals (6 weeks).

[43] *Weeks* [1993] pointed out that the friction coefficient for steady state given by *Dietrich* [1979] and *Ruina* [1983] may not be accurate at higher slip rate, and modified it to

$$\mu_{ss} = \mu_0 + a \ln\left(\frac{v}{v_0}\right) + b \ln\left(\frac{v_0}{v} + \frac{v_0}{v_T}\right) \tag{6}$$

where v_T is called transition velocity. This friction has a negative slope on stress-log(slip rate) plane at low slip rates when $a - b < 0$, but the slope becomes positive for slip rates greater than v_T. In appropriate circumstances, slip accelerates at $v < v_T$ and may decelerate at $v > v_T$, possibly producing an accelerating slip with sliding velocities significantly smaller than seismic velocities [*Weeks*, 1993]. *Shibazaki and Iio* [2003] performed a three dimensional simulation using Dietrich-Ruina friction law with a small cutoff velocity to an evolution effect in the friction law at depths below seismogenic zone and were able to reproduce slow slip events. However, *Liu and Rice* [2005] question whether there is an experimental basis for such a velocity cutoff.

[44] *Kilgore et al.* [1993] showed an increase in steady state friction with slip rate for granite only for the lowest normal stress (~5MPa), which would require near lithostatic pore pressure. In addition, their results were obtained at a slip rate of ~1 mm/s, which is much faster than the inferred slip rate of $<5 \times 10^{-9}$ m/s for the Tokai slow event.

[45] Among models in the second category, *Yoshida and Kato* [2003] considered two coupled spring sliders to

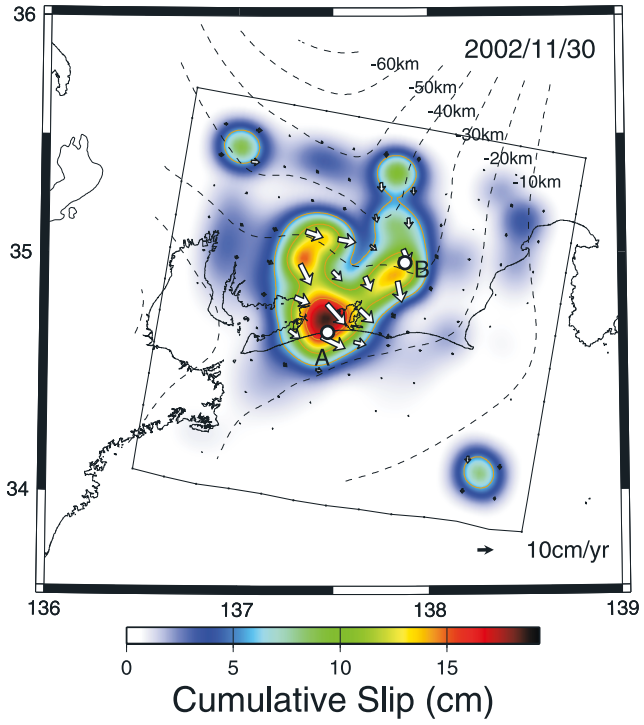

Figure 12. Cumulative slip inferred from the extended Network Inversion Filter. Arrows show the direction and magnitude of slip of the upper plate. A and B are specific points where the slip rate, slip, and stress change are shown in Figure 13.

simulate dynamic interactions. They assumed that the first slider had intrinsically unstable friction and varied the frictional parameters of only the second slider. They found that slow slip can occur when the second slider is conditionally stable. Notable features in their results are that the first slow event occurs long after the large stick slip of the first slider, and that slow events occur multiple times during the interseismic period of the first slider, but the peak slip rate (and stress drop) of the second slider decreases with time following a high-velocity slip event of the first slider [see, e.g., *Yoshida and Kato*, 2003, Figure 2]. This suggests that the stress-log(slip rate) paths becomes "stable spirals." *Liu and Rice* [2005] conducted three dimensional simulations of shallow subduction earthquakes based on rate-state friction with small along-strike variations in the constitutive parameters a and $(a - b)$. They found that slow slip emerged spontaneously around the downdip end of the seismogenic zone, where the frictional properties transition from steady state velocity weakening to velocity strengthening. They conclude that this transition in frictional properties together with the heterogeneous stress distribution, introduced either by spatial variations in the constitutive parameters or by heterogeneous initial conditions, are necessary for the occurrence of slow slip events.

[46] An important difference between the two mechanisms is the following: The first mechanism involves velocity weakening where the slow events nucleate, so that instabilities occur spontaneously. it involves a temporal change in the frictional behavior at a point. The second mechanism on the other hand, involves spatial variations in the frictional parameters and, according to *Liu and Rice* [2005], some degree of along-strike stress heterogeneity. That stress heterogeneity could result in part from large fast

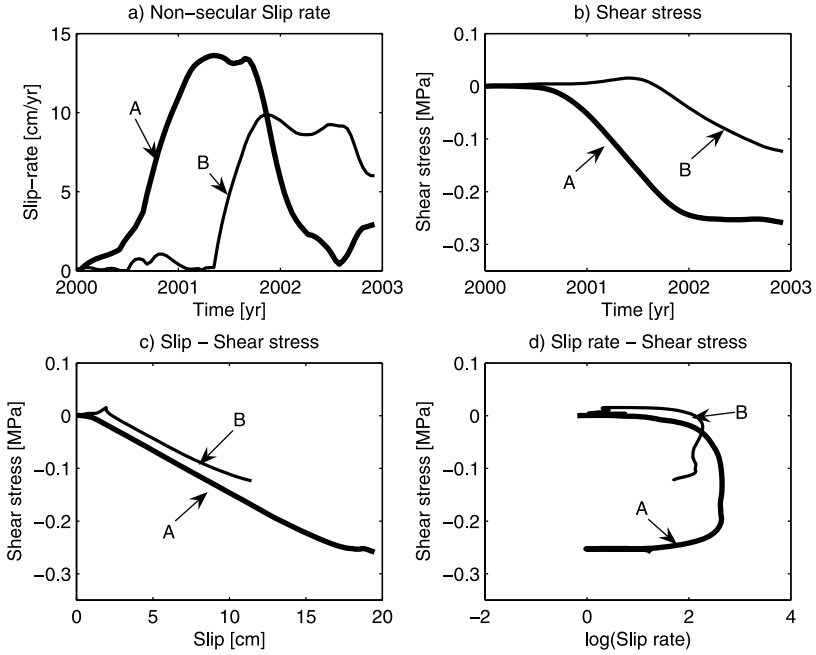

Figure 13. Slip, slip rate, and shear stress change at selected points on the fault (A, B shown in Figure 1 and Figure 12). (a) Transient slip rate history; (b) stress change history; (c) stress change as a function of slip; and (d) stress change as a function of log(slip rate). The unit of slip rate is in *cm/yr*.

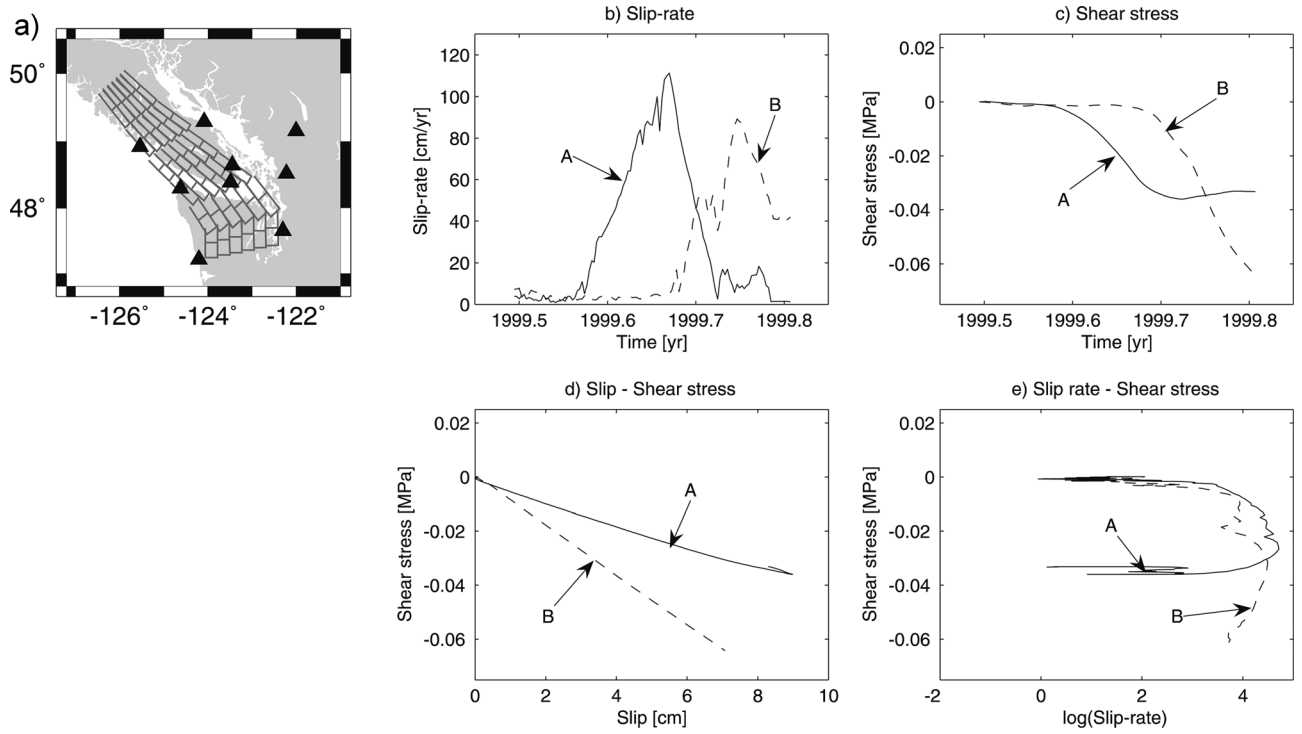

Figure 14. Slip, slip rate, and shear stress change at selected points on the fault for the 1999 Cascadia slow event. (a) Fault geometry for Cascadia (modified from *McGuire and Segall* [2003]); (b) slip rate history; (c) stress change history; (d) stress change as a function of slip; and (e) stress change as a function of log(slip rate). The unit of slip rate is in cm/yr.

slip events, however the slow slip events nucleate long after the earthquakes, so that the response to stress perturbation in this case is different from the case of the afterslip which initiates immediately after large earthquakes.

[47] Is it possible to know whether the slow slip area is frictionally unstable or conditionally stable? One key might lie in the stress-log(slip rate) paths. The paths for the *Yoshida and Kato* [2003] simulations should be stable spirals while the paths for the first are approximately cyclic (''limit cycles''). Hence, although we do know the appropriate phase space interpretation for continuum models such as *Liu and Rice* [2005], given data for multiple slow slip cycles, as in Cascadia, we might be able to distinguish between the two possibilities.

[48] The recent detection of low-frequency tremors in the Tokai area [*Ohta et al.*, 2004], as was previously found in Cascadia [*Rogers and Dragert*, 2003] and the Bungo Channel [*Obara et al.*, 2004], is suggestive of the involvement of pore fluids, and in any case is an essential clue which will ultimately be critical in understanding these events.

7. Discussion

7.1. Causal Relation Between the Tokai Slow Slip and the Miyake-jima Eruption

[49] The change of the Coulomb Failure Function on the Tokai subduction interface associated with Miyake-Kozu events is estimated to be on the order of 0.1 kPa beneath Lake Hamana, where slow slip nucleated. This stress step is significantly smaller than the secular stressing rate on the order of 10 kPa/yr. Hence it is unlikely that the Miyake-jima eruption triggered the Tokai slow slip event. However, since the coincidence in time is still intriguing, we examined whether the slow slip initiated before the onset of the Miyake-jima eruption from the slip histories obtained from the forward filter run (without backward smoothing) in two areas, one where the first subevent initiated (area a in Figures 1 and 15), the second where the second subevent

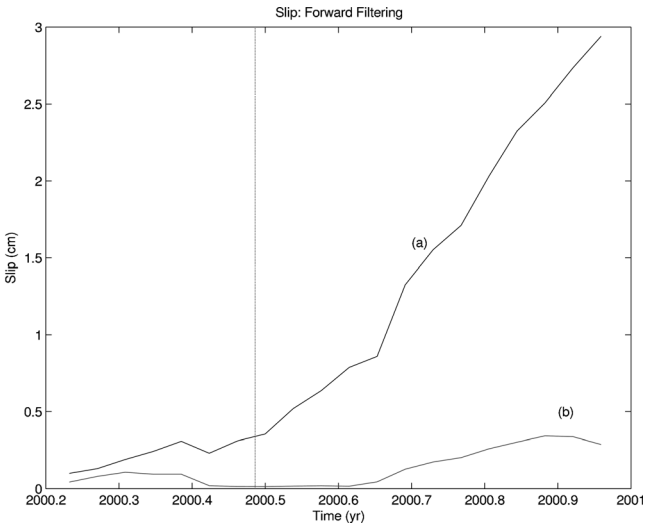

Figure 15. Averaged cumulative slip in areas a and b, shown in Figure 1, obtained by the forward filtering (without backward smoothing). The thick and thin lines show slip history in areas a and b, respectively. The vertical line shows the time of the onset of eruption (t = 2000.4863).

nucleated (area b in Figures 1 and 15). Focusing on the forward filter results avoids smearing of the signal in time associated with back smoothing [*Murray and Segall*, 2005] because, by definition, the filtered state at $t = t_k$, $X_{k|k}$, are obtained from data between the first epoch and the kth epoch. The slip in area a appears to accelerate prior to late June, when the eruption occurred, reaching an average slip of slightly less than 5 mm. While this does not exceed the formal uncertainties ($\sim$1 cm) it is substantially more than the inferred slip in the adjacent area, which is less than 2 mm, indicating that slip in the nucleation zone of the first subevent prior to the eruption is significant. Thus, while we cannot disprove triggering by the Miyake-jima eruption, it appears that the slow slip event nucleated prior to the volcanic activity.

7.2. Implications for the Occurrence of the Future Tokai Earthquake

[50] Comparing the slip distribution of the slow event (Figure 12) with the secular backslip distribution (Figure 4c), we found that the slow event occurred in a weakly coupled zone, probably transitional from the locked seismogenic zone to the freely sliding zone. Little slip was found in the area with backslip greater than 2 cm/yr. This result suggests that a future large earthquake might be promoted by the 2000 Tokai slow slip event. Hence we calculate the change in Coulomb Failure Function due to the slow slip event on the Suruga-Nankai Trough. Although the obtained distribution is rough, ΔCFF is a few to a few tens of kPa in the hypothesized Tokai earthquake region. This may be large enough to modulate the secular stress buildup of a few tens of kPa/yr.

8. Conclusion

[51] We inverted GPS time series in the Tokai area, central Japan. We inferred temporal and spatial variations of the ongoing Tokai slow slip event with an extended Network Inversion Filter. This event appears to have initiated slightly before the 2000 Miyake-Kozu eruption (early 2000), and involved two subevents. The first locus of slip at 137.4°E, 34.7°N accelerated in early to mid-2001 and decelerated at the end of 2001. A second locus at 137.7°E, 34.9°N initiated in late 2001, and accelerated in the following several months. This event is still ongoing, with a total duration of longer than 4 years.

[52] The stress-log(slip rate) paths are similar to those inferred for high speed ruptures with a limiting velocity of roughly 0.1 m/yr, which implies steady state velocity weakening including spontaneous slip nucleation or interaction of different frictional regions including conditionally stable ones. We found the same behavior in the 1999 Cascadia slow slip event with a limiting velocity of roughly 1 m/yr. The change in the Coulomb failure function due to the slow event suggests that the likelihood of a hypothesized Tokai earthquake is increased.

[53] **Acknowledgments.** We thank GSI for providing GPS data, T. Nishimura for providing his results. Critical reviews by an anonymous Associate Editor, two anonymous reviewers, and K. Johnson and proofreading by A. Hooper, J. Murray, and E. Desmarais improved the manuscript. Part of this study is supported by JSPS Postdoctral Fellowships for Research Abroad.

References

Akaike, H. (1980), Likelihood and the Bayes procedure, in *Bayesian Statistics*, edited by J. M. Bernardo et al., pp. 143–166, Univ. Press, Valencia, Spain.

Ando, M. (1975), Source mechanisms and tectonic significance of historical earthquakes along the Nankai Trough, Japan, *Tectonophysics*, *27*, 119–140.

Central Disaster Management Council (2001), The Central Disaster Management Council of the Japanese government, Tokyo. (Available at http://www.bousai.go.jp/jishin/chubou/20011218/siryou2-2.pdf)

Cervelli, P., P. Segall, K. Johnson, M. Lisowski, and A. Miklius (2002), Sudden aseismic fault slip on the south flank of Kilauea volcano, *Nature*, *415*, 1014–1018.

Dietrich, J. H. (1978), Time-dependent friction and the mechanics of stick slip, *Pure Appl. Geophys.*, *116*, 790–806.

Dietrich, J. H. (1979), Modeling of rock friction 1. Experimental results and constitutive equations, *J. Geophys. Res.*, *84*, 2161–2168.

Dong, D., T. A. Herring, and R. W. King (1998), Estimating regional deformation from a combination of space and terrestrial geodetic data, *J. Geod.*, *72*, 200–214.

Dragert, H. K., K. Wang, and T. S. James (2001), A silent slip event on the deeper Cascadia subduction interface, *Science*, *292*, 1525–1527.

El-Fiky, G., and T. Kato (2000), Study of periodic vertical movement in the Omaezaki peninsula, central Japan, and its tectonic implications, *Earth Planets Space*, *52*, 25–35.

Freymuller, J., S. Hreinsdottir, C. Zweck, and P. S. Haeussler (2002), The 1998–2002 deep megathrust slip event, Alaska, *Eos Trans. AGU*, *83*(47), Fall Meet. Suppl., Abstract G61-A-0972.

Fukahata, Y., A. Nishitani, and M. Matsu'ura (2004), Geodetic data inversion using ABIC to estimate slip history during one earthquake cycle with viscoelastic slip-response functions, *Geophys. J. Int.*, *156*, 140–153.

Fukuda, J. (2003), A new approach to time dependent inversion of geodetic data using Monte Carlo mixture Kalman Filter, Master thesis, 91 pp., Univ. of Tokyo, Tokyo.

Geographical Survey Institute (2003), Crustal deformation in Tokai District, *Rep. 69*, pp. 303–393, Coord. Comm. for Earthquake Predict., Tsukuba.

Geographical Survey Institute (2004), Crustal movements of Tokai Province (in Japanese), Tsukuba. (Available at http://cais.gsi.go.jp/tokai/)

Guatteri, M., P. Spudich, and G. Beroza (2001), Inferring rate and state friction parameters from a rupture model of the 1995 Hyogo-ken Nanbu (Kobe) Japan earthquake, *J. Geophys. Res.*, *106*, 26,511–26,522.

Hatanaka, Y., T. Iizuka, M. Sawada, A. Yamagiwa, Y. Kikuta, J. M. Johnson, and C. Rocken (2003), Improvement of the analysis strategy of GEONET, *Bull. Geogr. Surv. Inst.*, *49*, 11–37.

Heki, K., and S. Miyazaki (2001), Plate convergence and long-term crustal deformation in central Japan, *Geophys. Res. Lett.*, *28*, 2313–2316.

Heki, K., S. Miyazaki, H. Takahashi, M. Kasahara, F. Kimata, S. Miura, N. F. Vasilenko, A. Ivashchenko, and K.-D. An (1999), The Amurian Plate motion and current plate kinematics in eastern Asia, *J. Geophys. Res.*, *104*, 29,147–29,156.

Hirose, H., K. Hirahara, F. Kimata, N. Fujii, and S. Miyazaki (1999), A slow thrust slip event following the two 1996 Hyuganada earthquakes beneath the Bungo Channel, southwest Japan, *Geophys. Res. Lett.*, *26*, 3237–3240.

Ide, S., and M. Takeo (1997), Determination of constitutive relations of fault slip based on seismic wave analysis, *J. Geophys. Res.*, *102*, 27,379–27,392.

Ishibashi, K. (1981), Specification of a soon-to-occur seismic faulting in the Tokai district, central Japan, based upon seismotectonics, in *Earthquake Prediction: An International Review*, *Maurice Ewing Ser.*, vol. 4, edited by D. W. Simpson and P. G. Richards, pp. 297–332, AGU, Washington, D. C.

Ishida, M. (1992), Geometry and relative motion of the Philippine sea plate and Pacific plate beneath the Kanto-Tokai district, Japan, *J. Geophys. Res.*, *97*, 489–513.

Ito, T., and M. Hashimoto (2004), Spatiotemporal distribution of interplate coupling in southwest Japan from inversion of geodetic data, *J. Geophys. Res.*, *109*, B02315, doi:10.1029/2002JB002358.

Kato, N., and T. Hirasawa (1999), A model for possible crustal deformation prior to a coming large interplate earthquake in the Tokai district, central Japan, *Bull. Seismol. Soc. Am.*, *89*, 1401–1417.

Kilgore, B. D., M. L. Blanpied, and J. H. Dieterich (1993), elocity dependent friction of granite over a wide range of conditions, *Geophys. Res. Lett.*, *20*, 903–906.

Kimata, F., and T. Yamauchi (1998), Time series of line lengths on the baselines in the Tokai region detected by EDM in the period of 1978 to 1997 (in Japanese), J, *Seismol. Soc. Jpn., Extra Vol. Ser. 2*, *51*, 229–232.

Kostoglodov, V., S. K. Singh, J. A. Santiago, S. I. Franco, K. Larson, A. Lowry, and R. Bilham (2003), A large silent earthquake in the Guerrero

seismic gap, Mexico, *Geophys. Res. Lett.*, *30*(15), 1807, doi:10.1029/2003GL017219.
Kumagai, H. (1996), Time sequence and the recurrence models for large earthquakes along the Nankai Trough revisited, *Geophys. Res. Lett.*, *23*, 1139–1142.
Kuroki, H., H. M. Ito, and A. Yoshida (2002), A 3-D simulation of crustal deformation accompanied by subduction in the Tokai region, central Japan, *Phys. Earth Planet. Inter.*, *132*, 39–58.
Larson, K., V. Kostoglodov, A. Lowry, W. Hutton, O. Sanchez, K. Hudnut, and G. Suarez (2004), Crustal deformation measurements in Guerrero, Mexico, *J. Geophys. Res.*, *109*, B04409, doi:10.1029/2003JB002843.
Linde, A. T., M. T. Gladwin, M. J. S. Johnston, R. L. Gwyther, and R. G. Bilham (1996), A slow earthquake sequence near San Juan Bautista, California in December 1992, *Nature*, *383*, 65–69.
Liu, Y., and J. R. Rice (2005), Aseismic slip transients emerge spontaneously in three-dimensional rate and state modeling of subduction earthquake sequences, *J. Geophys. Res.*, *110*, B08307, doi:10.1029/2004JB003424.
Lowry, A., K. Larson, V. Kostoglodov, and R. Bilham (2001), Transient slip on the subduction interface in Guerrero, southern Mexico, *Geophys. Res. Lett.*, *28*(19), 3753–3756.
Matsumura, S. (1997), Focal zone of a future Tokai earthquake inferred from the seismicity pattern around the plate interface, *Tectonophysics*, *273*, 271–291.
McGuire, J., and P. Segall (2003), Imaging of aseismic slip transients recorded by continuous GPS array, *Geophys. J. Int.*, *155*, doi:10.1111/j.1365-246X.2003.02022.x.
Mikumo, T., K. B. Olsen, E. Fukuyama, and Y. Yagi (2003), Stress-breakdown time and slip-weakening distance inferred from slip-velocity functions on earthquake faults, *Bull. Seismol. Soc. Am.*, *93*, 264–282.
Miller, M. M., T. Melbourne, D. J. Johnson, and W. Q. Summer (2002), Periodic slow earthquakes from the Cascadia subduction zone, *Science*, *295*, 2423.
Miyazaki, S., and K. Heki (2001), Crustal velocity field of Southwest Japan: Subdution and arc-arc collision, *J. Geophys. Res.*, *106*, 4305–4326.
Miyazaki, S., T. Saito, M. Sasaki, Y. Hatanaka, and Y. Iimura (1997), Expansion of GSI's nationwide GPS array, *Bull. Geogr. Surv. Inst.*, *43*, 23–34.
Miyazaki, S., J. J. McGuire, and P. Segall (2003), A transient subduction zone slip episode in southwest Japan observed by the nationwide GPS array, *J. Geophys. Res.*, *108*(B2), 2087, doi:10.1029/2001JB000456.
Munekane, H., M. Tobita, and K. Takashima (2004), Groundwater-induced vertical movements observed in Tsukuba, Japan, *Geophys. Res. Lett.*, *31*, L12608, doi:10.1029/2004GL020158.
Murray, J. R., and P. Segall (2005), Spatiotemporal evolution of a transient slip event on the San Andreas fault near Parkfield, California, *J. Geophys. Res.*, *110*, B09407, doi:10.1029/2005JB003651.
Nishimura, T., S. Ozawa, M. Murakami, T. Sagiya, T. Tada, M. Kaidzu, and M. Ukawa (2001), Crustal deformation caused by magma migration in the northern Izu Islands, Japan, *Geophys. Res. Lett.*, *28*, 3745–3748.
Obara, K., H. Hirose, F. Yamamizu, and K. Kasahara (2004), Episodic slow slip events accompanied by non-volcanic tremors in southwest Japan subduction zone, *Geophys. Res. Lett.*, *31*, L23602, doi:10.1029/2004GL020848.
Ohta, Y., F. Kimata, and T. Sagiya (2004), Reexamination of the interplate coupling in the Tokai region, central Japan, based on the GPS data in 1997–2002, *Geophys. Res. Lett.*, *31*, L24604, doi:10.1029/2004GL021404.
Okada, Y. (1992), Internal deformation due to shear and tensile faults in a half-space, *Bull. Seismol. Soc. Am.*, *82*, 1018–1040.
Ozawa, S., M. Murakami, and T. Tada (2001), Time-dependent inversion study of the slow thrust event in the Nankai Trough subduction zone, southwestern Japan, *J. Geophys. Res.*, *106*, 787–802.
Ozawa, S., M. Murakami, M. Kaidzu, T. Tada, T. Sagiya, Y. Hatanaka, H. Yarai, and T. Nishimura (2002), Detection and monitoring of ongoing aseismic slip in the Tokai region, central Japan, *Science*, *298*, 1009–1012, doi:10.1126/science.1076780.
Ozawa, S., S. Miyazaki, T. Nishimura, M. Murakami, M. Kaidzu, T. Imakiire, and X. Ji (2004a), Creep, dike intrusion, and magma chamber deflation model for the 2000 Miyake eruption and the Izu islands earthquakes, *J. Geophys. Res.*, *109*, B02410, doi:10.1029/2003JB002601.
Ozawa, S., Y. Hatanaka, M. Kaidzu, M. Murakami, T. Imakiire, and Y. Ishigaki (2004b), Aseismic slip and low-frequency earthquakes in the Bungo channel, southwestern Japan, *Geophys. Res. Lett.*, *31*, L07609, doi:10.1029/2003GL019381.
Rice, J. R., and A. L. Ruina (1983), Stability of steady frictional slipping, *J. Appl. Mech.*, *50*, 343–349.
Rice, J. R., and S. T. Tse (1986), Dynamic motion of a single degree of freedom system following a rate and state dependent friction law, *J. Geophys. Res.*, *91*, 521–530.
Rogers, G., and H. Dragert (2003), Episodic tremor and slip on the Cascadia subduction zone: The chatter of silent slip, *Science*, *300*, 1942–1943.
Ruina, A. (1983), Slip instability and state variable friction laws, *J. Geophys. Res.*, *88*, 10,359–10,370.
Sagiya, T. (1999), Interplate coupling in the Tokai district, central Japan, deduced from continuous GPS data, *Geophys. Res. Lett.*, *26*, 2315–2318.
Sangawa, A. (1993), The paleo-earthquake study using traces of the liquefaction (in Japanese), *Quat. Res.*, *32*, 249–255.
Savage, J. C. (1983), A dislocation model of strain accumulation and release at a subduction zone, *J. Geophys. Res.*, *88*, 4984–4996.
Segall, P., and R. Harris (1987), Earthquake deformation cycle on the San Andreas fault near Parkfield, California, *J. Geophys. Res.*, *92*, 10,511–10,525.
Segall, P., and M. Matthews (1997), Time dependent inversion of geodetic data, *J. Geophys. Res.*, *102*, 391–409.
Seno, T., S. Stein, and A. E. Gripp (1993), A model for the motion of the Philippine Sea plate consistent with NUVEL-1 and geological data, *J. Geophys. Res.*, *98*, 17,941–17,948.
Shibazaki, B., and Y. Iio (2003), On the physical mechanism of silent slip events along the deeper part of the seismogenic zone, *Geophys. Res. Lett.*, *30*(9), 1489, doi:10.1029/2003GL017047.
Simon, D., and D. L. Simon (2003), Aircraft turbofan engine health estimation using constrained Kalman filtering, paper presented at ASME Turbo Expo 2003, Atlanta, Ga.
Toda, S., R. S. Stein, and T. Sagiya (2002), Evidence from the AD 2000 Izu islands earthquake swarm that stressing rate governs seismicity, *Nature*, *419*, 58–61.
Weeks, J. D. (1993), Constitutive laws for high-velocity frictional sliding and their influence on stress drop during unstable slip, *J. Geophys. Res.*, *98*, 17,637–17,648.
Yabuki, T., and M. Matsu'ura (1992), Geodetic data inversion using a Bayesian information criterion for spatial distribution of fault slip, *Geophys. J. Int.*, *109*, 363–375.
Yamazaki, F., and H. Aoki (1994), Re-examination of the configuration of the PHS plate—Is the slab continuous or discontinuous?, paper presented at 1994 Japan Earth and Planetary Science Joint Meeting, Sendai, Japan.
Yoshida, S., and N. Kato (2003), Episodic aseismic slip in a two-degree-of-freedom block-spring model, *Geophys. Res. Lett.*, *30*(13), 1681, doi:10.1029/2003GL017439.
Yoshioka, S., T. Mikumo, V. Kostoglodov, K. M. Larson, A. Lowry, and S. K. Singh (2004), Interplate coupling and a recent aseismic slow slip event in the Guerrero seismic gap of the Mexican subduction zone, as deduced from GPS data inversion using a Bayesian information criterion, *Phys. Earth Planet. Inter.*, *146*(3–4), 513–530.

Y. Hatanaka, Geographical Survey Institute, Tsukuba, 305-0811, Japan. (hata@gsi.go.jp)
T. Kato and S. Miyazaki, Earthquake Research Institute, University of Tokyo, Tokyo, 113-0032, Japan. (teru@eri.u-tokyo.ac.jp; miyazaki@eri.u-tokyo.ac.jp)
J. J. McGuire, Woods Hole Oceanographic Institution, Woods Hole, MA 02543, USA. (jmcguire@whoi.edu)
P. Segall, Department of Geophysics, Stanford University, Stanford, CA 94304, USA. (segall@stanford.edu)